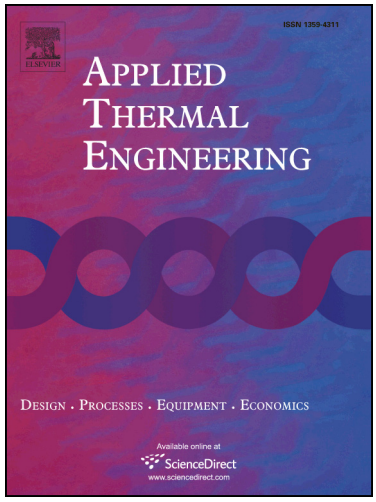

Research Paper

Performance and Potential Energy Saving of Thermal Dryer with Intermittent Impinging Jet

Jundika C. Kurnia, Agus P. Sasmito, Peng Xu, Arun S. Mujumdar

PII: S1359-4311(16)33071-X
DOI: http://dx.doi.org/10.1016/j.applthermaleng.2016.11.036
Reference: ATE 9446

To appear in: *Applied Thermal Engineering*

Received Date: 29 August 2016
Revised Date: 27 October 2016
Accepted Date: 5 November 2016

Please cite this article as: J.C. Kurnia, A.P. Sasmito, P. Xu, A.S. Mujumdar, Performance and Potential Energy Saving of Thermal Dryer with Intermittent Impinging Jet, *Applied Thermal Engineering* (2016), doi: http://dx.doi.org/10.1016/j.applthermaleng.2016.11.036

Performance and Potential Energy Saving of Thermal Dryer with Intermittent Impinging Jet

Jundika C Kurnia[1*], Agus P Sasmito[2†], Peng Xu[3], Arun S Mujumdar[2,4]

[1]Department of Mechanical Engineering, Universiti Teknologi PETRONAS, 32610 Bandar Seri Iskandar, Perak Darul Ridzuan, Malaysia

[2]Department of Mining and Materials Engineering, McGill University, 3450 University, Frank Dawson Adams Bldg., Montreal, QC, H3A2A7 Canada

[3]College of Science, China Jiliang University, 258 Xueyuan Street, Hangzhou 310018, PR China

[4]School of Food Science, University of Queensland, Brisbane, Australia

Abstract

In designing an energy efficient impinging jet dryer, it is essential to match the energy demand for drying with the supply of heat by convection to avoid overheating and energy wastage. One way to achieve this is by intermittently supply heat to the drying chamber. By using computational fluid dynamics (CFD) approach, this study numerically investigates the possibility of energy saving by intermittency. First, inlet temperature intermittency is applied. This is conducted by alternately raise it to drying temperature and lowers it to the ambient temperature at certain period. Second, inlet velocity intermittency is applied which is conducted by alternately supplying the hot air to the several drying chamber. One, two, three and four chamber configurations are evaluated. In addition, the intermittency period of 10, 20 and 30 minutes were examined. The results reveal that the steady impinging jet offers faster drying rate as compared to intermittent impinging jet drying under the same inlet conditions. In addition it was found that drying rate goes down as the number of drying chamber increases. However, the intermittent impinging jet drying offers advantages in term of

* Email: kurnia.jc@gmail.com; jundika.kurnia@utp.edu.my; Phone: +605 368 7157
† Email: agus.sasmito@mcgill.ca

temperature uniformity and energy conservation. For the same energy usage, the production rate of single drying configuration is only one fourth of the four chamber configuration. This indicates the potential of multi chamber configuration in a real drying application.

Keywords: energy saving, intermittent impinging jet, numerical study, performance evaluation, thermal drying.

1. Introduction

For industrial drying operation which requires short drying time, impinging jet of various configurations is preferred. It is particularly desirable to dry flat and thin product such as tissue paper, coated paper, tiles, textiles, wood veneer, lumber and carpet [1]. Impinging jet offers high heat and mass transfer rate [2,3] which is essential in drying as drying rate is dictated by the rate of heat and mass transfer occurs within the drying substrate and in the surrounding. Despite their potential, designing impinging jet dryer is challenging, considering the complexity of various transport processes and interactions that occur simultaneously during drying. Therefore, understanding of the fundamental of heat and mass transfer and effect of various parameters on the drying performance is essential.

In effort to elucidate basic mechanisms of impinging jet drying, numerous experimental and numerical investigations have been conducted and reported. Ratanawilai et al. [4] investigated drying characteristic of rubber wood in dryer with combination of impinging jet hot air and microwave heating. It was found that impinging jet increase the drying rate and significantly reduce the drying time. Nuntadusit and Waehahyee [5] evaluated impinging jet drying system for rubber sheet. They developed the dryer using an array of hot air jet in staggered arrangement impinging on both side of the rubber. The results indicated that impingement is not beneficial for all cases as drying rate is controlled by rubber properties. The performance of impinging jet drying on a moving plate was studied by Bai et al. [6].

Several key parameters affecting the heat and moisture transfer performance were evaluated. Etemoglu and Can [7] evaluated thermal performance of single and multiple impinging jet system with various size, shapes and configurations. Based on their evaluation, for drying application three parameters are important, i.e. nozzle height, nozzle size and nozzle pitch. Summary of the effect of various design parameters (e.g. type of nozzle, nozzle array arrangement, nozzle diameter) on the performance of impinging jet drying has also been reported [8].

While having impressive drying performance, the application of steady impinging jet for drying is hindered by its inherent drawbacks of higher energy consumption as compared to traditional parallel flow drying and high possibility of burning product due to over-heating. Hence, it is crucial to match the heat supply to the heat required for drying to obtain an optimum drying process – high transfer rate, minimum energy consumption and high quality dried product. One way to achieve it is by supplying heat to the drying process periodically or intermittently according to the needs of the drying application; for example, pulsating and intermittent heat supply. The benefits of pulsating and intermittent flow in heat transfer applications (heating, cooling and drying) have been reported by several researchers. Islam et al. [9] numerically investigated intermittency in temperature, velocity and relative humidity for parallel flow dryer. It was found that intermittency is potential for energy saving while maintaining good drying performance. Xu et al. [10,11] carried out numerical simulation on the intermittent impinging jet and reported significant heat transfer enhancement by intermittent pulsation. Yahyaee et al [12] conducted numerical study of the motion and drying characteristic of wet particle in a pulsed opposing jet contactor (POJC). POJC was found promising for particulate heat transfer and drying. Panao et al [13] highlighted in their article that intermittent spray cooling is beneficial for intelligent thermal management. Intermittency was also applied for cryogenic spray cooling using liquid nitrogen to achieve

the required operating temperature which otherwise difficult to achieve with steady flow [14]. On drying application, Kurnia et al [15] reported that impinging jet drying with pulsation and intermittent flow offers promising energy saving while having comparable drying performance as those with steady flow. In the reported study, however, only one intermittent configuration was evaluated: intermittency of inlet velocity 1 on 1 off. There are several possible configurations that have not been evaluated and will be beneficial if carefully examined.

The objective of the current study is therefore to numerically evaluate drying performance and potential energy saving of thermal drying with impinging jet with various intermittent configurations by utilizing computational fluid dynamics (CFD) approach. First, intermittent of inlet temperature is introduced by alternately raising and lowering the temperature of supplied drying air (hot and cold jet). In this configuration, the drying air is steady supplied to the drying chamber. To further reduce the energy usage, inlet velocity intermittency is implemented by alternately supplying hot drying air to several drying chambers. Several possible intermittent scenarios will be evaluated: one chamber (steady jet), two chambers (intermittent 1 on 1 off), three chambers (intermittent 1 on 2 off) and four chambers (intermittent 1 on 3 off) configurations. The effect of intermittency period will be investigated as well. The drying performance in term of drying rate and potential energy savings will be evaluated in the light of numerical result.

2. Model formulation

The mathematical model is based on the validated model in our previous study [15]: A slice of potato is dried inside a drying chamber under a slot impinging jet, as illustrated in Figure 1. Simultaneous transport phenomena occurring in this process are:

- Diffusion of water moisture from the inner drying substrate to its surface

- Convection from drying air to the surface of drying substrate
- Conduction within the drying substrate
- Evaporation and convection of vapor from the surface of drying substrate to the drying air.

Due to its complex nature, several assumptions are required to develop the model:

- The drying substrate is homogeneous and it has uniform initial temperature and moisture content.
- Inside the drying substrate, water vapor diffuses significantly faster than liquid water. Moisture transfer is modeled as diffusive process.
- The properties of the drying substrate are isotropic and dependent of temperature and moisture content.
- The properties of drying air are temperature-dependent.
- Due to the slenderness of the drying substrate, variation of dependent variables in span wise direction is assumed to be negligible. Hence the process can be treated as two-dimensional problem.
- Neither shrinkage nor deformation is considered in this study.

2.1. Governing equations

Based on the given assumptions, the conservation of mass and energy inside the drying substrate, accounting for both water vapor and liquid water, can be expressed as [15, 16]

$$\frac{\partial c_l}{\partial t} + \nabla \cdot \left(- D_{l_b} \nabla c_l \right) = -K c_l , \tag{1}$$

$$\frac{\partial c_v}{\partial t} + \nabla \cdot \left(- D_{vb} \nabla c_v \right) = K c_v , \tag{2}$$

$$\rho_b c_{pb} \frac{\partial c_v}{\partial t} + \nabla \cdot \left(- k_b \nabla T \right) = -\dot{q}. \tag{3}$$

Here, c_l is the liquid water concentration, c_v is the water vapor concentration, D_{lb} and D_{vb} are the liquid water and water vapor diffusivities in the drying substrate, respectively. T is temperature, $\dot{q}$ is the evaporation induced cooling rate, K is the water vapor production rate, ρ_b is the drying substrate density, c_{pb} is drying substrate specific heat and k_b is the drying substrate heat conductivity.

Meanwhile, conservation of mass, momentum and energy as well as conservation of vapor species in the drying air are given by [10, 15]

$$\nabla \cdot \mathbf{u} = 0, \tag{4}$$

$$\rho_a \left(\frac{\partial \mathbf{u}}{\partial t} + \mathbf{u} \nabla \mathbf{u} \right) = -\nabla p + \nabla \left(\mu \nabla \mathbf{u} - \rho_a \overline{\mathbf{u}'} \right), \tag{5}$$

$$\rho_a c_{pa} \left(\frac{\partial T}{\partial t} + \nabla \mathbf{u} T \right) = \nabla \cdot \left(k_a \nabla T - \rho_a c_{pa} \overline{\mathbf{u}' T'} \right), \tag{6}$$

$$\frac{\partial c_v}{\partial t} + \nabla \cdot \left(- D_{va} \nabla c_v \right) = -\mathbf{u} \nabla c_v, \tag{7}$$

where $\mathbf{u}$ is the air mean velocity, $\mathbf{u}'$ is the air fluctuate velocity, p is pressure, μ is the air dynamic viscosity, ρ_a is the drying air density, c_{pa} is the drying air specific heat, k_a is the drying air thermal conductivity, and D_{va} is the water vapor diffusivity in the drying air.

Similar to our previous study [15], the Reynolds Stress Model [17] is implemented to take into account the turbulent flow of the drying air, i.e.

$$\frac{\partial R_{ij}}{\partial t} + C_{ij} = P_{ij} + D_{ij} - \varepsilon_{ij} + \Pi_{ij} + \Omega_{ij}, \tag{8}$$

where

$$\frac{\partial Rij}{\partial t}=\frac{\partial\left(\rho_a \overline{u_i' u_j'}\right)}{\partial t}, C_{ij}=\nabla\cdot\left(\rho_a \overline{u_i' u_j'}\mathbf{U}\right), P_{ij}=-\left(R_{im}\frac{\partial U_j}{\partial X_m}+R_{jm}\frac{\partial U_i}{\partial X_m}\right), Dij=\nabla\cdot\left(\frac{\mu t}{\sigma k}\nabla R_{ij}\right)$$

$$\varepsilon_{ij}=\frac{2}{3}\varepsilon\delta_{ij}, \Pi_{ij}=-C_1\frac{\varepsilon}{k}\left(R_{ij}-\frac{2}{3}k\delta_{ij}\right)-C_2\frac{\varepsilon}{k}\left(P_{ij}-\frac{2}{3}P\delta_{ij}\right), \Omega ij=-2\omega k\left(\overline{u_j' u_m'}e_{ikm}+\overline{u_i' u_m'}e_{jkm}\right)$$

$$\text{and } \mu_t=C_\mu\frac{k2}{\varepsilon}, \tag{9}$$

are the accumulation, convective, production, diffusion, dissipation, pressure-strain interaction and rotation terms, respectively. The variables R_{ij}, δ_{ij}, C_μ, σ_k, C_1 and C_2 are the Reynolds stress tensor, Kronecker delta and constants whose values are given in Table 1. The turbulent kinetic energy k and turbulent dissipation ε in the above equation can be found by solving k-ε turbulent model [17], i.e.

$$\frac{\partial}{\partial t}(\rho k)+\nabla\cdot(\rho\mathbf{u}k)=\nabla\cdot\left[\left(\mu+\frac{\mu_t}{\sigma_k}\right)\nabla k\right]+G_k-\rho\varepsilon, \tag{10}$$

$$\frac{\partial}{\partial t}(\rho\varepsilon)+\nabla\cdot(\rho\mathbf{u}\varepsilon)=\nabla\cdot\left[\left(\mu+\frac{\mu_t}{\sigma_\varepsilon}\right)\nabla\varepsilon\right]+C_{1\varepsilon}\frac{\varepsilon G_k}{k}+C_{2\varepsilon}\rho\frac{\varepsilon^2}{k}, \tag{11}$$

where G_k is the generation of turbulence kinetic energy due to the mean velocity gradients, $C_{1\varepsilon}$ and $C_{2\varepsilon}$ are constants, σ_k and σ_ε are the turbulent Prandtl numbers for k and ε, respectively. The turbulent viscosity is given by $\mu_t=\rho C_\mu k^2/\varepsilon$.

2.2. Constitutive relations

In this study, polynomial functions are adopted to represent temperature dependent properties of drying air which were obtained from Kays et al. [18]. The drying air properties are summarized in Table 2 together with the properties for drying substrate.

As that in our previous study [15], the concept of vapor rate production [16] is adopted in this study. To account for water depletion in the drying substrate, a negative source term, Kc_l, is introduced to the conservation equation of liquid water (Eq. 1) whereas a positive source term is incorporated in the conservation equation of water vapor (Eq. 2) to take into account water vapor production inside the drying substrate. The rate of water vapor production is represented by an Arrhenius-type function, i.e.

$$K = K_0 e^{\frac{-E_a}{RT}}, \tag{12}$$

where K_0 is constant, E_a is the activation energy and R is the universal gas constant. Meanwhile the rate of cooling due to evaporation, $\dot{q}$, is given by

$$\dot{q} = \Delta h_{evap} M_l K c_l. \tag{13}$$

Here, M_l, is the molar mass of water, Δh_{evap} is total heat of evaporation which is given by

$$\Delta h_{evap} = h_{fg} + H_w \tag{14}$$

where h_{fg} is latent heat of evaporation and H_w is the heat of wetting which is the heat needed to evaporate the bound water. Correlations of both are presented in Table 2.

The dry basis moisture content, X, is defined as

$$X = \frac{m_{water}}{m_{dry}} = \frac{\rho_l}{\rho_s}. \tag{15}$$

and is related to the wet basis moisture content, W, by

$$W = \frac{m_{water}}{m_{wet}} = \frac{\rho_l}{\rho_b} = \frac{\rho_l}{\rho_s + \rho_l} = \frac{X}{1+X}. \tag{16}$$

By substituting density of drying substrate into the definition of wet basis moisture content, a relation between moisture content and water concentration inside the drying substrate can be obtained, i.e.

$$\left(S_b - \frac{\rho_{b,ref}}{M_l c_l}\right)X^2 + \left(S_b + 1 - \frac{\rho_{b,ref}}{M_l c_l}\right)X + 1 = 0. \quad (17)$$

This quadratic equation can be solved to obtain the root which provides the expression for moisture content [15]. Similar to study by Chemki et al. [19], to calculate the equilibrium moisture content, Guggenheim-Andersson-deBoer (GAB) equation is used.

The total energy consumption is calculated as the total of energy for pumping and heating the drying air within one hour.

$$E_{total} = P_{pump} + \dot{Q}_{heating} \quad (18)$$

The former is calculated as power required to drive the drying air, i.e.

$$P_{pump} = \frac{1}{\eta_{pump}}\dot{V}\Delta p, \quad (19)$$

while the later is the energy needed to raise the temperature of drying air from ambient temperature to the drying temperature given by

$$\dot{Q}_{heating} = \dot{m}_a c_p (T_{in} - T_{amb}), \quad (20)$$

where η_{pump} is pump efficiency (assumed to be 70%), $\dot{V}$ is the volumetric flow rate, T_{in} and T_{amb} are the jet inlet and ambient temperature (taken to be 298.15 K), respectively. Mass flow rate of drying air, $\dot{m}$, is calculated as

$$\dot{m}_a = \rho_a A_c v_{in} \quad (21)$$

where v_{in} is the inlet velocity. To evaluate and compare energy usage for each drying scenario, a parameter called ratio required energy is defined as the ratio between the energy

usages of each scenario as compared to that of steady set which is chosen as the benchmark, i.e.

$$\text{Ratio required energy} = \frac{\text{Total energy consumption of each case}}{\text{Total energy consumption of steady jet}} \tag{22}$$

2.3. Initial and boundary conditions

The initial conditions for drying substrate are:

$$T = T_0,\ c_l = c_{l0,b},\ c_v = c_{v0,b}. \tag{23}$$

Meanwhile, the initial conditions for drying are

$$T = T_0,\ c_l = c_{l0,a},\ c_v = c_{v0,a},\ u = v = 0. \tag{24}$$

whose values are summarized in Table 1. The required boundary conditions to solve the model are summarized as follows

- Inlet

$$u = 0,\ v = v_{in},\ T = T_{in},\ RH = RH_{in},\ c_v = c_{v0,a}. \tag{25}$$

- Outlet

$$p = p_{out},\ \mathbf{n}\cdot\left(-D\nabla c_v\right) = 0,\ \mathbf{n}\cdot\left(-D\nabla T\right) = 0. \tag{26}$$

- Wall

$$u = v = 0,\ \mathbf{n}\cdot\left(-D\nabla c_v\right) = 0,\ \mathbf{n}\cdot\left(-D\nabla T\right) = 0. \tag{27}$$

- Coupled boundary condition was set at drying substrate/air interface

$$u = v = 0,\ T\big|_{-} = T\big|_{+},\ c_v\big|_{-} = c_v\big|_{+}. \tag{28}$$

Here, **n** is unit vector normal to the given surface, $|_-$ and $|_+$ denote condition inside and outside the drying substrate.

2.4. Numerical methodology

The computational domain was created, meshed and labeled in Gambit preprocessor software (please refer to Fig. 1 for the computational domain representation). Before proceeding into the studied cases, a mesh independent test was conducted by systematically doubling the amount of mesh; starting from 0.5×10^3, 1×10^3, 2×10^3, 4×10^3 and 8×10^3 elements. It was found that mesh size amounting 4×10^3 elements differs by less than 2% as compared to mesh size of 8×10^3 elements with respect to drying rate, while it differs by more than 8%, 12% and 20% as compared to mesh size of 2×10^3, 1×10^3 and 0.5×10^3 elements, respectively. Thus, it can be deduced that mesh size of 4×10^3 is sufficient for our purpose. A fine structured mesh was implemented on the inlet, impinging region and drying substrate to capture the impinging jet flow and the corresponding heat and mass transfer. Meanwhile, to optimize the computational resources and time, an increasingly coarser mesh is applied towards the outlet.

The mathematical model (Eqs. 1-11), together with constitutive relations and boundary conditions are solved by utilizing ANSYS Fluent 15. ANSYS user-defined function (UDF) written in C language is incorporated to take into account the temperature dependency of drying air and drying substrate thermal properties. User-defined scalar (UDS) and user-defined memory (UDM) functionalities are utilized to account for moisture content within the drying substrate and drying air. The model was solved with Semi-Implicit Pressure-Linked Equation (SIMPLE) algorithm, second order upwind discretization and Algebraic Multi-grid (AMG) method. A convergence criterion of 10^{-4} was set for conservation of mass and 10^{-6} for other parameters. For 4 hours simulated drying time, approximately 12-14 hours simulation time is required on a personal computer with 2.0 GHz quad processor and 6 GB RAM.

3. Results and discussion

A typical drying condition, as summarized in Table 3, was numerically simulated in this study. Before proceeding towards investigation of intermittency, model validation is conducted and is presented in the following section.

3.1. Model validation

The current model is based on the model developed in our previous study [19] which has been validated against the experimental data by Islam et al [9]. To provide better overview, the validation is re-presented in Fig. 2. Overall, the model predictions achieve good agreement with the experimental measured counterpart over the entire period of drying, providing evidence on the validity of the model. The model is then utilized to investigate the drying performance and potential energy saving of thermal drying with impinging jet with various intermittent configurations.

3.2. Inlet temperature intermittency

As stated previously, the steady impinging jet has inherent drawback of higher energy consumption and higher possibility of overheating which will lead to product damage (burnt). Hence, it is crucial to match the heat supplied with the demand for optimal drying. Here, the drying air is supplied steadily but the temperature is alternately changed between 298.15 K (25°C) and 318.15 K (45°C) Fig. 3 presents drying kinetics of impinging jet with steady and intermittent inlet temperature. As can be observed, steady jet offers faster drying compared with that of intermittent jet under the same inlet condition. This is expected since for the intermittent temperature cases, the drying substrate will be alternately exposed to cold and hot air. When cold air is supplied, the temperature of the drying substrate will reduce, leading to a slower evaporation and thus slower drying. Subsequently, when the hot air is supplied,

the drying substrate will take some time to reach the temperature for the evaporation to take place, resulting in a longer drying time. The reduction in drying rate is more prominent for intermittent with longer "off" period. This is most likely attributed to the longer cooling period which brings down the drying substrate temperature to a lower level, thus lengthen the required re-heating period.

Looking into the effect of intermittent period, as presented in Fig. 4, it can be seen that the intermittent period play marginal role in determining the drying rate even though on closer inspection it is clear that longer intermittent period is beneficial in securing faster drying. For all studied cases, the intermittent period of 30 mins offers faster drying as compared to the shorter intermittent period. It may be due to the fact that the drying substrate require some time during re-heating process to reach optimum temperature for evaporation. With shorter intermittent period, this condition may have not been achieved when the changes in drying air temperature take place.

Despite the weakness in term of slower drying, intermittent temperature has advantages of lower substrate temperature during drying, minimizing the possibility of burning the product due to overheating. This lower temperature is also beneficial for drying of temperature sensitive products, such as pharmaceutical products. Figs 5 and 6 present temperature and moisture content distribution in drying substrate for steady and intermittent temperature jet, respectively. As can be inferred, steady velocity jet reaches higher drying substrate temperature which may not be desirable as it can lead to overheating and thus reducing the quality of the drying product. On the other hand, intermittent jet yields lower temperature where longer "off" period results in even lower product temperature. Closer inspection reveals that, on average, about 6 ºC temperature difference is noticed between steady temperature and intermittent 1-on-1-off. While lesser temperature difference of about 3 ºC

and 1 ºC is observed for 1-on-2-off and 1-on-3-off designs, respectively. Clearly, careful consideration on cooling period has to be taken though as too low temperature may drag the drying time even longer. Another consideration which need to be taken into account is the cooling temperature, it may be better if the cooling temperature is increased little bit such that the optimum evaporation point can be achieved faster while maintaining the product temperature below overheating condition. This study will be conducted in the near future.

3.3 Inlet velocity intermittency

In previous section, the heating energy has been alternately supplied to the drying air to reduce energy usage. To minimize energy consumption even further, the drying air is alternately supplied to several drying chambers instead of single drying chamber. As stated previously 4 different scenarios are investigated: (*i*) steady jet which correspond to single chamber configuration, (*ii*) 1 on 1 off intermittent jet which correspond to 2 drying chamber configuration where the hot drying air is alternately supplied to chamber 1 and chamber 2 with interval of 1/2 period (1/2 τ), (*iii*) 1 on 2 off intermittent jet which represent 3 drying chamber configuration where at every 1/3 period (1/3 τ) only 1 chamber is supplied with hot drying air (on) while the other 2 chamber are not supplied (off), (*iv*) 1 on 3 off intermittent jet which correspond to 4 drying chamber configuration where hot drying air is alternately supplied to each chamber with interval of 1/4 period (1/4 τ). The considered velocity intermittent scenarios are presented in Fig 7. The drying kinetics of impinging jet with intermittent inlet velocity is presented in Fig. 8. In-line with the finding for intermittent temperature, the steady jet offers faster drying. However, the difference in drying rate for steady and intermittent velocity is not as large as those in intermittent temperature cases. This is most likely attributed to the fact that in this case the cooling process is slower as compared to the intermittent temperature where the drying substrate is blown with cold air. Hence the

re-heating process is faster, thus leading to faster drying than those of intermittent temperature.

Turning our attention towards the effect of intermittent period on drying kinetics, as presented in Fig. 9, we found similar trend with the previous cases where the effect of period is marginal. On closer observation, however, it was found that, in contrast to intermittent temperature cases, longer intermittent period result in slower drying. This is attributed to the fact that in intermittent temperature, air is steadily supplied albeit at lower temperature. Hence transfer of water vapor from the substrate to the drying air is remaining. In contrast, in intermittent velocity, air is alternately supplied. As such the longer the period of intermittency, the slower mass transfer occurs from the substrate to the drying air. This is somewhat beneficial to the drying quality as the moisture has sufficient time to diffuse throughout the substrate which, in turn, gives rise to a more uniform temperature and moisture distribution. In some heat sensitive materials, the uniformity of temperature and moisture can be of importance due to the fact that it affects structural deformation and thus final product quality.

Fig. 10 presents temperature distribution in drying substrate for steady and intermittent velocity jet, respectively. Similar to intermittent temperature cases, steady velocity jet (one chamber) reaches higher temperature and intermittent jet yields lower temperature where dryer with more chamber results in lower temperature. As compared to intermittent temperature cases, higher temperature is observed for intermittent velocity. This is mainly attributed to the fact that in intermittent case during drying hot and cold air are supplied alternately. During cold air impingement, cooling process take place, reducing the substrate temperature. Accordingly, lower moisture content is observed for the intermittent velocity cases, as illustrated in Fig. 11. This is due to higher temperature of the substrate in

intermittent velocity cases, providing sufficient driving force for moisture content evaporation. For intermittent temperature cases, on contrary, low temperature hinder the evaporation process and thus slower the drying.

3.4 Energy savings

Thus far, the drying performance of various intermittency configuration and scenario has been evaluated. Here, the energy consumption and potential energy saving arising from intermittent drying with jet impingement is quantified and examined. The overall energy consumption figure for the studied cases is presented in Fig. 12. The energy consumption is calculated for 1 hour time frame for which the intermittent period has no effect on the calculation. The energy consumption for steady flow is set as a benchmark for this assessment. The energy consumption for steady flow is attributed from fan pumping power (78 J/h) and heater (642 kJ/h). This figure implies that the dominant energy consumption is heating of drying air.

From the figure, it is clear that intermittency offers considerable reduction on energy consumption. Furthermore, higher energy saving can be obtain by increasing the number of drying chambers. Notably about 50%, 67% and 75% energy savings can be obtained for two, three and four chambers arrangement, respectively. The potential of energy savings of up to 75% for four chambers arrangement together with more uniform moisture content distribution show potential for practical/industrial application of the multiple chamber arrangement at a cost of longer drying time (~1.6 times longer). Clearly, optimization between design and operating parameters is required to obtain optimum drying performance.

4. Conclusions

A computational investigation on the effect of intermittency of inlet temperature and velocity on the drying kinetics of an impinging jet system is reported. The drying performances of steady and intermittent impinging jets have been compared with each other, and the effect of intermittent period on the drying rate has been discussed. The numerical results indicate that the steady impinging jet offers faster drying rate compared with intermittent impinging jet drying under same inlet conditions, and longer intermittent temperature period and shorter intermittent velocity period can slightly increase drying rate. However, the intermittent impinging jet drying indicate advantages in temperature uniformity and energy conservation, which indicates the potential of multi chamber configuration in a real drying application. An important note is that during cooling process, the temperature of the substrate may be too low which result is slower re-heating and in turn slower drying. Continuation study will be conducted to investigate the effect of cold air temperature on the drying performance and energy saving.

NOMENCLATURES

c	Concentration	mol m^{-3}
c_p	Specific heat	J kg^{-1} K^{-1}
D	Diffusivity	m^2 s^{-1}
E_a	Activation energy	J mol^{-1}
h_{fg}	Latent heat of evaporation	J kg^{-1}
H_w	Heat of wetting	J kg^{-1}
k	Thermal conductivity	W m^{-2} K^{-1}
K	Water vapor production rate	s^{-1}
K_0	Constant of water vapor production rate	s^{-1}
M	Molar mass	kg mol^{-1}
n	Normal vector	-

p	Pressure	Pa
$\dot{q}$	Cooling rate due to evaporation	W m^{-3}
R	Universal gas constant	J K^{-1} mol^{-1}
T	Temperature	K
u, u, v	Velocity	m s^{-1}
X	Dry basis moisture content	kg kg^{-1}
X_e	Equilibirum moisture content	kg kg^{-1}
W	Wet basis moisture content	kg kg^{-1}
Greek letter		
ρ	Density	kg m^3
μ	Dynamic viscosity	Pa s
Δh_{evap}	Total heat of evaporation	J kg^{-1}
τ	Intermittent period	min
Subscript		
0	Initial condition	
a	Drying air	
amb	Ambient	
b	Drying substrate	
in	Inlet	
l	Liquid water	
out	Outlet	
v	Water vapor	

REFERENCES

[1] A.S. Mujumdar, Handbook of Industrial Drying, CRC Press, Boca Raton, Florida, 2007.

[2] P. Forooghi, B. Frohnapfel, F. Magagnato, Simulation of a gaseous jet impinging on a convex heated surface – effect of inlet condition, Appl. Therm. Eng. 105 (2016) 1076-1084.

[3] R. Vinze, S. Chandel, M.D. Limaye, S.V. Prabhu, Effect of compressibility and nozzle configuration on heat transfer by impinging air jet over a smooth plate, Appl. Therm. Eng. 101 (2016) 293-307.

[4] T. Ratanawilai, C. Nuntadusit, N. Promtong, Drying characteristics of rubberwood by impinging hot air and microwave heating, Wood Res. 60 (2015) 59-70.

[5] C. Nuntadusit, M. Waehahyee, Drying of rubber sheet using impingement of multiple hot air jets, Adv. Mater. Res. 844 (2014) 502-506.

[6] G.P. Bai, G.C. Gong, F.Y. Zhao, Z.X. Lin, Multiple thermal and moisture removals from the moving plate opposing to the impinging slot jet, Appl. Therm. Eng. 66 (2014) 252-265.

[7] A.B. Etemoglu, M. Can, Performance studies of energy consumption for single and multiple mozzle systems under impinging air jets, Heat Mass Transfer 49 (2013) 1057-1070.

[8] E. Specht, Impinging jet drying, In: E. Tsotsas, A.S. Mujumdar (Eds.), Modern Drying Technology Volume 5, Process Intensification. Wiley-VCH Velag, Weinheim Germany, 2014, pp. 1-26.

[9] M.R. Islam, J.C. Ho, A.S. Mujumdar, Convective drying with time-varying heat input, Simulation results. Dry. Technol. 21 (2003) 1333-1356.

[10] P. Xu, B. Yu, S. Qiu, H.J. Poh, A.S. Mujumdar, Turbulent impinging jet heat transfer enhancement due to intermittent pulsation, Int. J. Therm. Sci. 49 (2010) 1247-1252.

[11] P. Xu, S. Qiu, M. Yu, X. Qiao, A.S. Mujumdar, A study on the heat and mass transfer properties of multiple pulsating impinging jets, Int. Commun. Heat Mass 39 (2012) 378-382.

[12] A. Yahyaee, K. Esmailpour, M. Hosseinalipour, A.S. Mujumdar, Simulation of drying characteristics of evaporation from a wet particle in a turbulent pulsed opposing jet contactor, Dry. Technol. 31 (2013) 1994-2006.

[13] M.R.O Panao, A.M. Correira, A.L.N. Moreira, High-power electronics thermal management with intermittent multijet sprays, Appl. Therm. Eng. 37 (2012) 293-301.

[14] S. Somasundaram, A.A.O. Tay, A study of intermittent liquid nitrogen sprays, Appl. Therm. Eng. 69 (2014) 199-207.

[15] J.C. Kurnia, A.P. Sasmito, W. Tong, A.S. Mujumdar, Energy-efficient thermal drying using impinging-jets with time varying heat input - A computational study, J. Food Eng. 114 (2013) 269-277.

[16] M.V. De Bonis, G. Ruocco, A generalized conjugate model for forced convection drying based on an evaporative kinetics, J. Food Eng. 89 (2008), 232-240.

[17] D.C. Wilcox, Turbulence modeling for CFD. DCW Industries, La Canada, California, 2006.

[18] W. Kays, M. Crawford B. Weigand Convective Heat and Mass Transport, fourth ed. McGraw Hill, Singapore, 2005.

[19] S. Chemki, F. Zagrouba, A. Bellagi, Mathematical model for drying of highly shrinkable media, Dry. Technol. 22 (2004) 1023-1039.

[20] J. Srikiatden, J.S. Roberts, Predicting moisture profiles in potato and carrot during convective hot air drying using isothermally measured effective diffusivity, J. Food Eng. 84 (2008) 516-525.

[21] Y.A. Cengel, A.J. Ghajar, Heat and Mass Transfer Fundamental and Applications, fifth ed. MacGraw Hill, Singapore, 2015.

[22] J.C. Kurnia, A.P. Sasmito, A.S. Mujumdar, Evaluation of heat transfer performance of helical coils of non-circular tubes. J. Zhejiang Univ-Sci. A (Appl. Phys. & Eng.) 12 (2011) 63-70.

[23] G. Nellis, S. Klein, Heat Transfer. Cambridge University Press, Cambridge, 2009.

Table and Figure Captions

Table 1 Geometry and operating parameters

Table 2 Properties of drying air and drying substrate (potato)

Table 3 Intermittency parameters

Fig. 1. (a) Schematic of multiple drying chambers configurations, (b) considered computational domain, and (c) mesh element of the computational domain.

Fig. 2. Validation of drying model with experimental data by Islam et al [9].

Fig. 3. Effect of inlet temperature intermittency on the drying kinetics (τ = 10 mins).

Fig. 4. Effect of period (τ) on the kinetics of impinging jet drying with intermittent inlet temperature: (a) intermittent 1 on 1 off, (b) intermittent 1 on 2 off, and (c) intermittent 1 on 3 off. Drying kinetics for steady jet is given as reference.

Fig. 5. Temperature distributions in drying substrate for steady and intermittent temperature jets (τ = 10 mins) at various time: (a) t = 30 mins, (b) 60 mins, (c) 120 mins and (d) 180 mins.

Fig. 6. Moisture content distributions in drying substrate for steady and intermittent temperature jets (τ = 10 mins) at various time: (a) t = 30 mins, (b) 60 mins, (c) 120 mins and (d) 180 mins.

Fig. 7. Various velocity intermittency scenarios and their corresponding drying chamber arrangements: (a) steady jet (single chamber), (b) 1 on 1 off intermittent jet (two chambers), (c) 1 on 2 off intermittent jet (three chambers) and (d) 1 on 3 off intermittent jet (4 chambers).

Fig. 8. Effect of inlet velocity intermittency on the drying kinetics (τ = 10 mins).

Fig. 9. Effect of period on the kinetics of impinging jet drying with intermittent inlet velocity: (a) intermittent 1 on 1 off, (b) intermittent 1 on 2 off, and (c) intermittent 1 on 3 off. Drying kinetics for steady jet is given as reference.

Fig. 10. Temperature distributions in drying substrate for steady and intermittent velocity jets (τ = 10 mins) at various time: (a) t = 30 mins, (b) 60 mins, (c) 120 mins and (d) 180 mins.

Fig. 11. Moisture content distributions in drying substrate for steady and intermittent velocity jets (τ = 10 mins) at various time: (a) t = 30 mins, (b) 60 mins, (c) 120 mins and (d) 180 mins.

Fig. 12. Energy consumptions of various intermittency scenarios

Table 2 Geometry and operating parameters

Parameter	Value	Unit	Reference
C_μ	0.09	-	[17]
σ_k	1.0	-	[17]
σ_ε	1.3	-	[17]
C_1	1.8	-	[17]
C_2	0.6	-	[17]
$C_{1\varepsilon}$	1.44	-	[17]
$C_{2\varepsilon}$	1.92	-	[17]
$c_{l0,b}$	$\frac{W_0 \rho_{b,ref}}{M_l}$	mol m^{-3}	[16]
$c_{v0,b}$	0	mol m^{-3}	[16]
$c_{l0,a}$	0	mol m^{-3}	[16]
$c_{v0,a}$	$1000\frac{RH\rho_{a,0}}{(1+RH)M_l}$	mol m^{-3}	[16]
X_0	4.6	kg kg^{-1}	[9]
$\rho_{b,ref}$	1420	kg m^{-3}	[20]
M_l	0.018	kg mol^{-1}	[21]
R	8.314	J K^{-1} mol^{-1}	[21]
S_b	1.4	-	[20]
K_0	7000	s^{-1}	[15]
E_a	48.7	kJ mol^{-1}	[16]
C	4.416	-	[19]
K_{GAB}	0.976	-	[19]
T_{in}	45	°C	-
RH_{in}	20	%	-

L	0.4	m	[15]
w	0.02	m	[15]
L_s	0.03	m	[15]
H_s	$5x10^{-3}$	m	[15]
w_j	$4x10^{-3}$	m	[15]
$\rho_{a,45°C}$	1.110	kg m^{-3}	[18]
$\mu_{a,45°C}$	1.934×10^{-5}	kg m^{-1} s^{-1}	[18]

Table 2 Properties of drying air and drying substrate (potato)

Property	Expression	Unit	Reference
ρ_a	$1.076\times10^{-5}T^2-1.039\times10^{-2}T+3.326$	kg m^{-3}	[18,22]
μ_a	$5.21\times10^{-15}T^3-4.077\times10^{-11}T^2+7.039\times10^{-8}T+9.19\times10^{-7}$	kg m^{-1} s^{-1}	[18,22]
k_a	$4.084\times10^{-10}T^3-4.519\times10^{-7}T^2+2.35\times10^{-4}T-0.0147$	W m^{-2} K^{-1}	[18,22]
$c_{p,a}$	$-4.67\times10^{-6}T^3+4.837\times10^{-3}T^2-1.599T+1175$	J kg^{-1} K^{-1}	[18,22]
ρ_b	$\frac{\rho_{b,re}f(1+X)}{1+SbX}$	kg m^{-3}	[20]
k_b	$\frac{0.049}{1+X}\exp\left[-\frac{47}{8.314\times10^{-3}}\left(\frac{1}{T}-\frac{1}{335.15}\right)\right]+\frac{0.611X}{1+X}$	W m^{-2} K^{-1}	[9]
$c_{p,b}$	$1750+2345\left(\frac{X}{1+X}\right)$	J kg^{-1} K^{-1}	[16]
D_{vb}=D_{lb}	$1.29\times10^{-6}\exp\left(-\frac{0.725}{X}\right)\exp\left(-\frac{2044}{T}\right)$,	m^2 s^{-1}	[9]
D_{va}	$1.656\times10^{-10}T^2+4.479\times10^{-8}T-2.775\times10^{-6}$.	m^2 s^{-1}	[23]
h_{fg}	$2.394T+2502.1$	kJ kg^{-1}	[9]
H_w	$8.327\times10^6X^4+4.0\times10^6X^3-6.161\times10^6X^2+2.368\times10^6X+1163\ (0.01<X<0.2)$.	kJ kg^{-1}	[9]
X_e	$\frac{X_mCK_{GAB}A_w}{(1-K_{GAB}A_w)(-K_{GAB}A_w+CK_{GAB}A_w)}$	kg kg^{-1}	[19]

Table 3 Intermittency parameters

Scenario	Inlet temperature intermittency	Inlet velocity intermittency
Single drying chamber (*Steady jet*)	$v_{in} = 2\ \mathrm{m\,s^{-1}}$ $T_{in} = 318.15\ \mathrm{K}$	$v_{in} = 2\ \mathrm{m\,s^{-1}}$ $T_{in} = 318.15\ \mathrm{K}$
Two drying chamber (*intermittent 1 on 1 off*)	$v_{in} = 2\ \mathrm{m\,s^{-1}}$ $T_{in} = \begin{cases} 318.15\ \mathrm{K} & \text{for } n\tau < t \le \left[\frac{1}{2}(2n+1)\right]\tau \\ 298.15\ \mathrm{K} & \text{for } \left[\frac{1}{2}(2n+1)\right]\tau < t \le (n+1)\tau \end{cases}$	$v_{in} = \begin{cases} 2\ \mathrm{m\,s^{-1}} & \text{for } n\tau < t \le \left[\frac{1}{2}(2n+1)\right]\tau \\ 0 & \text{for } \left[\frac{1}{2}(2n+1)\right]\tau < t \le (n+1)\tau \end{cases}$ $T_{in} = 318.15\ \mathrm{K}$
Three drying chamber (*intermittent 1 on 2 off*)	$v_{in} = 2\ \mathrm{m\,s^{-1}}$ $T_{in} = \begin{cases} 318.15\ \mathrm{K} & \text{for } n\tau < t \le \left[\frac{1}{3}(3n+1)\right]\tau \\ 298.15\ \mathrm{K} & \text{for } \left[\frac{1}{3}(3n+1)\right]\tau < t \le (n+1)\tau \end{cases}$	$v_{in} = \begin{cases} 2\ \mathrm{m\,s^{-1}} & \text{for } n\tau < t \le \left[\frac{1}{3}(3n+1)\right]\tau \\ 0 & \text{for } \left[\frac{1}{3}(3n+1)\right]\tau < t \le (n+1)\tau \end{cases}$ $T_{in} = 318.15\ \mathrm{K}$
Four drying chamber (*intermittent 1 on 3 off*)	$v_{in} = 2\ \mathrm{m\,s^{-1}}$ $T_{in} = \begin{cases} 318.15\ \mathrm{K} & \text{for } n\tau < t \le \left[\frac{1}{4}(4n+1)\right]\tau \\ 298.15\ \mathrm{K} & \text{for } \left[\frac{1}{4}(4n+1)\right]\tau < t \le (n+1)\tau \end{cases}$	$v_{in} = \begin{cases} 2\ \mathrm{m\,s^{-1}} & \text{for } n\tau < t \le \left[\frac{1}{4}(4n+1)\right]\tau \\ 0 & \text{for } \left[\frac{1}{4}(4n+1)\right]\tau < t \le (n+1)\tau \end{cases}$ $T_{in} = 318.15\ \mathrm{K}$

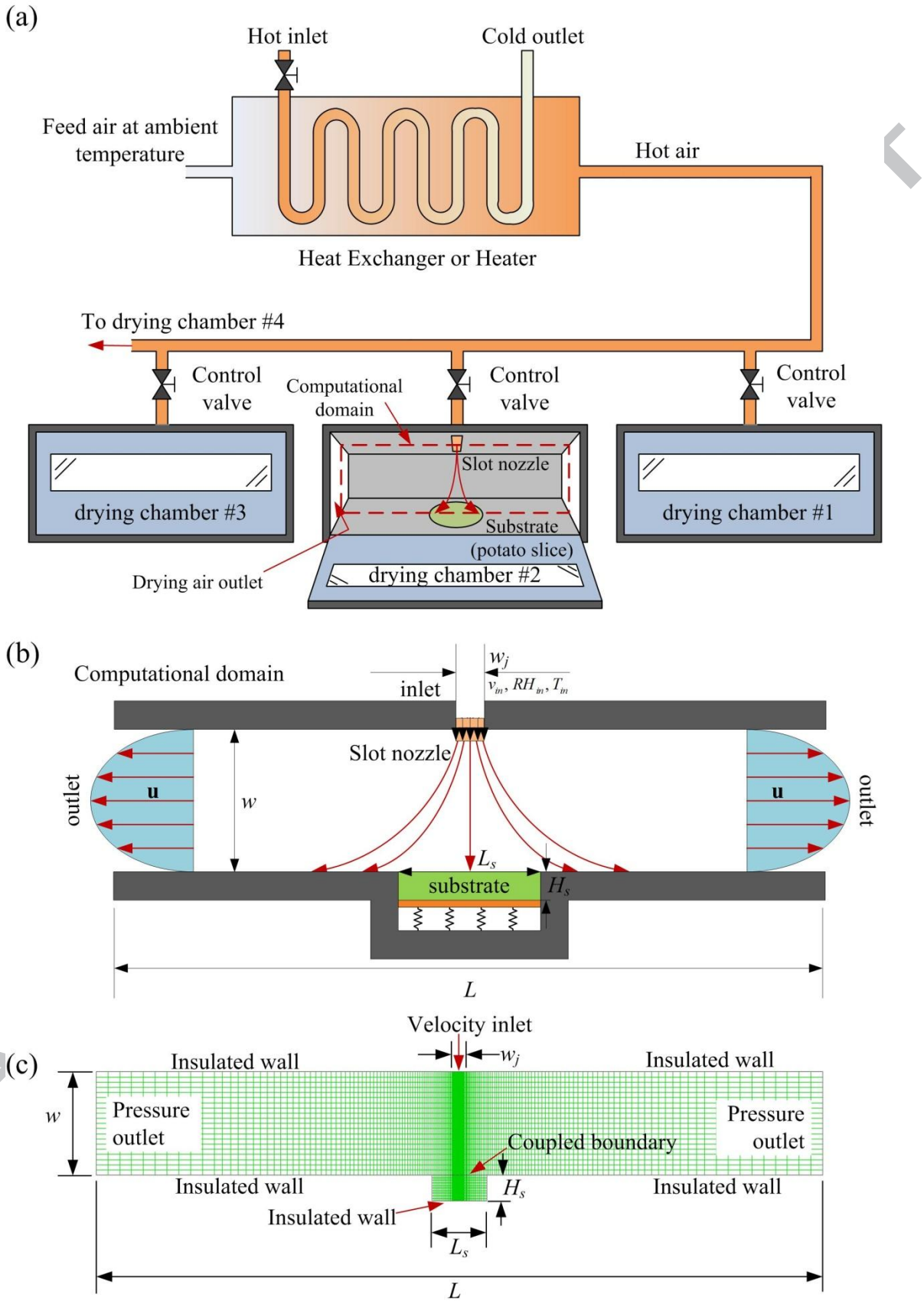

Fig. 1

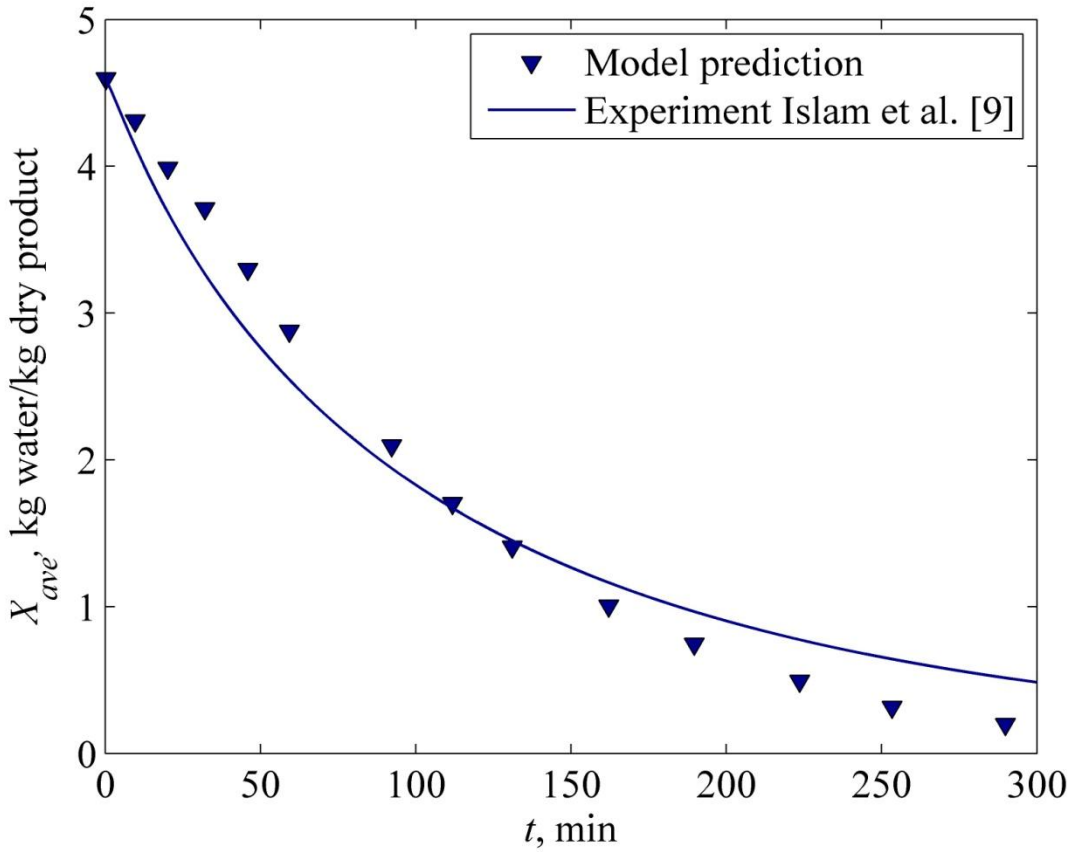

Fig. 2

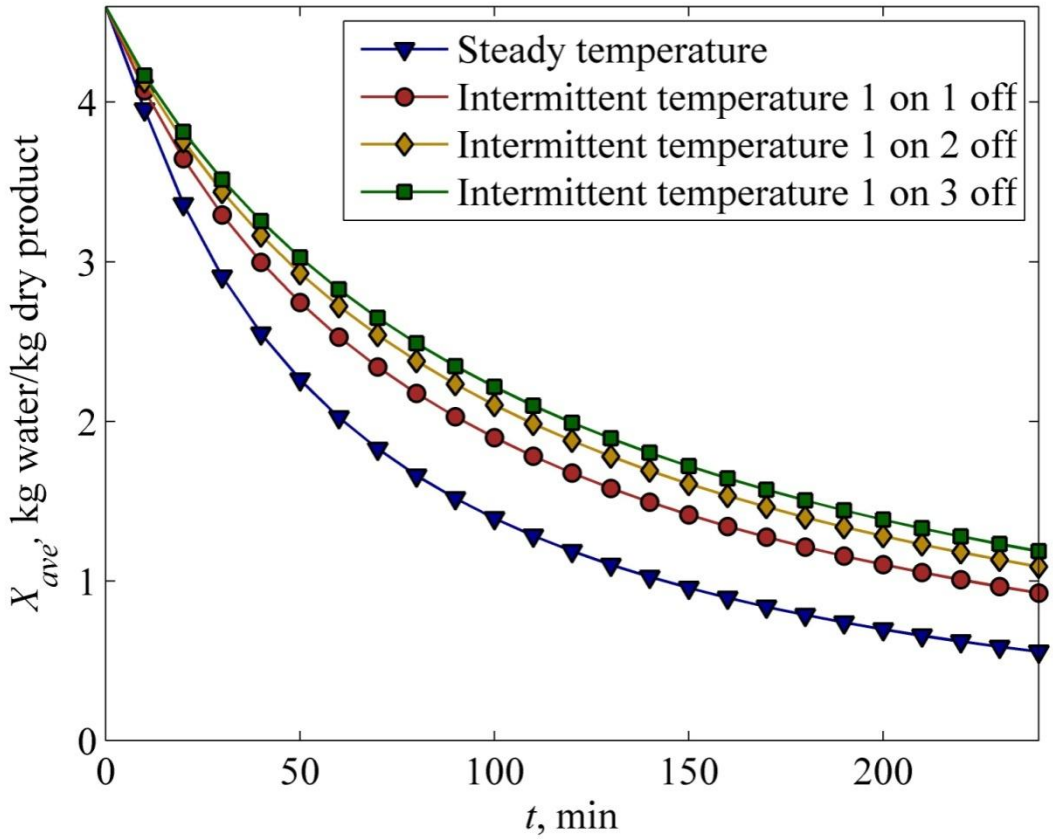

Fig. 3

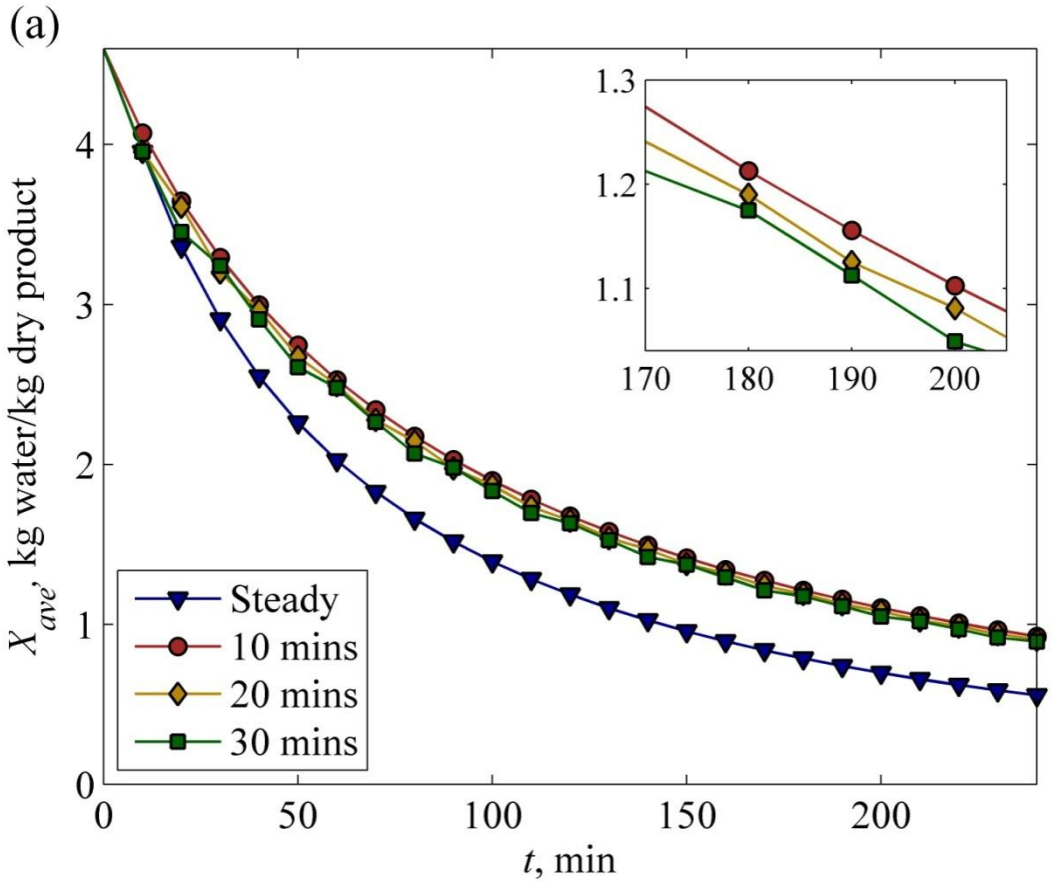
(a)
X_{ave}, kg water/kg dry product
t, min
Steady
10 mins
20 mins
30 mins

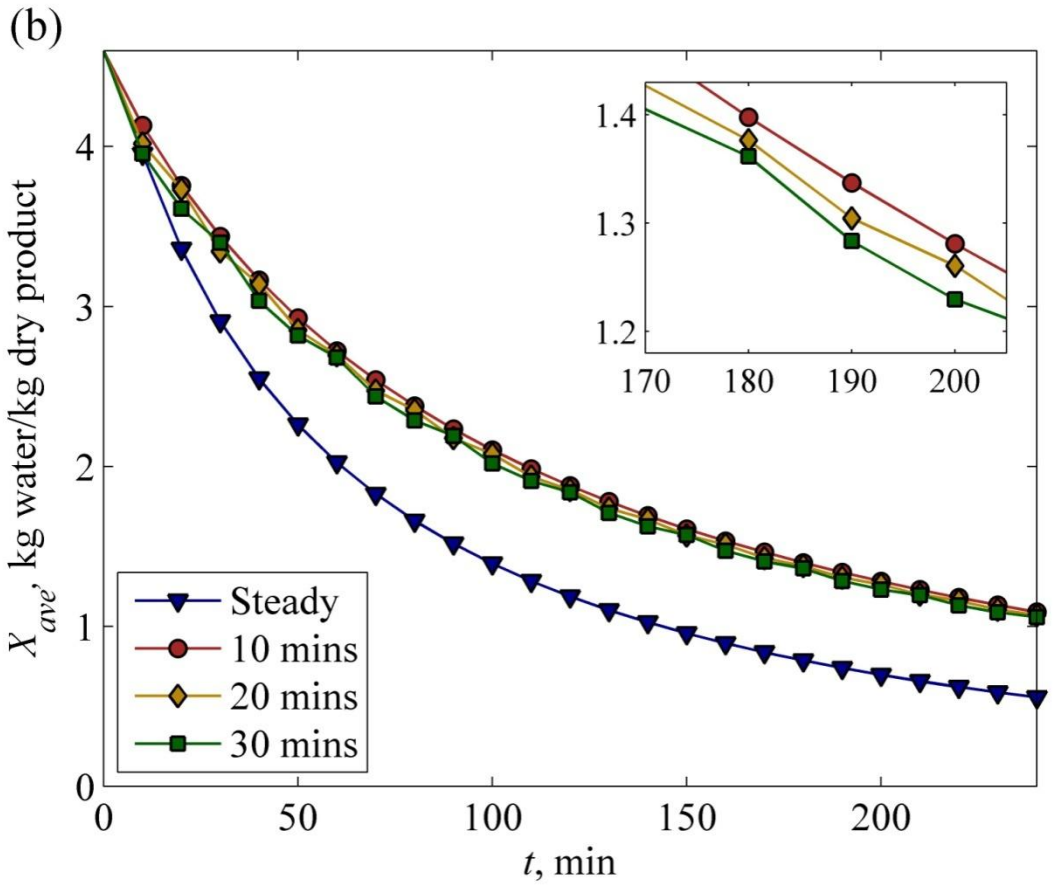
(b)
X_{ave}, kg water/kg dry product
t, min
Steady
10 mins
20 mins
30 mins

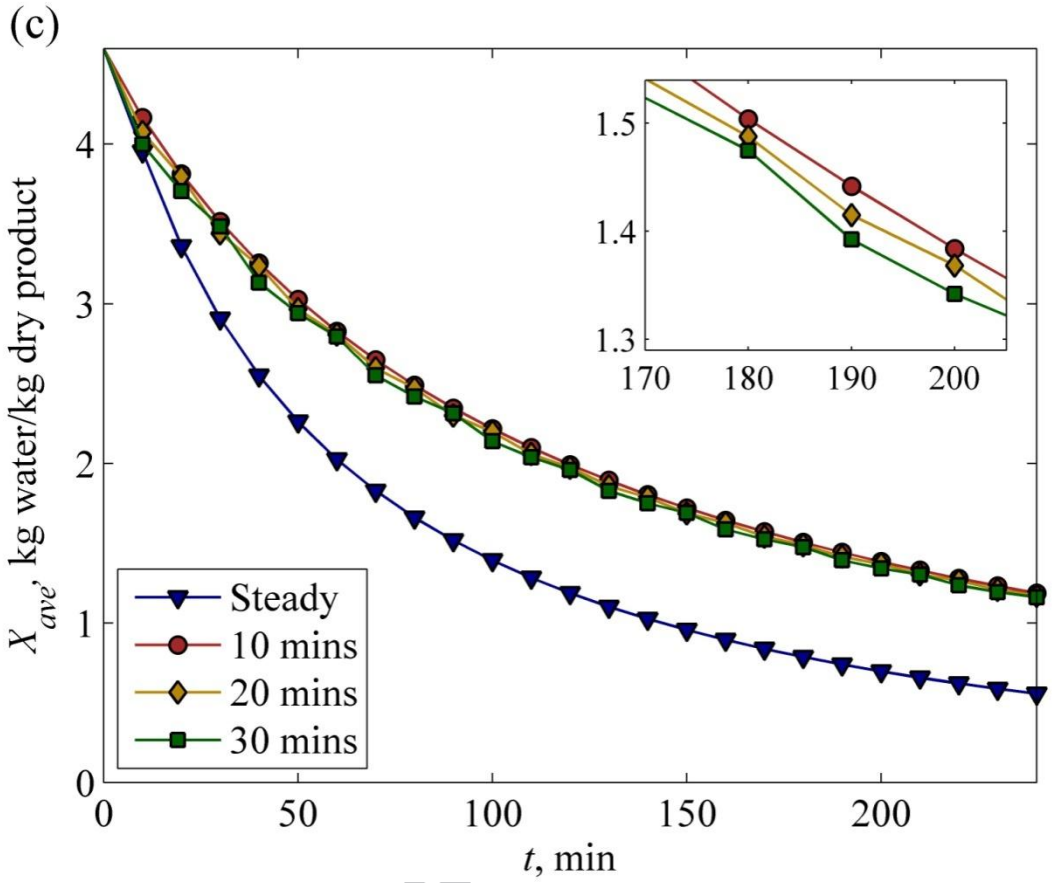

Fig. 4

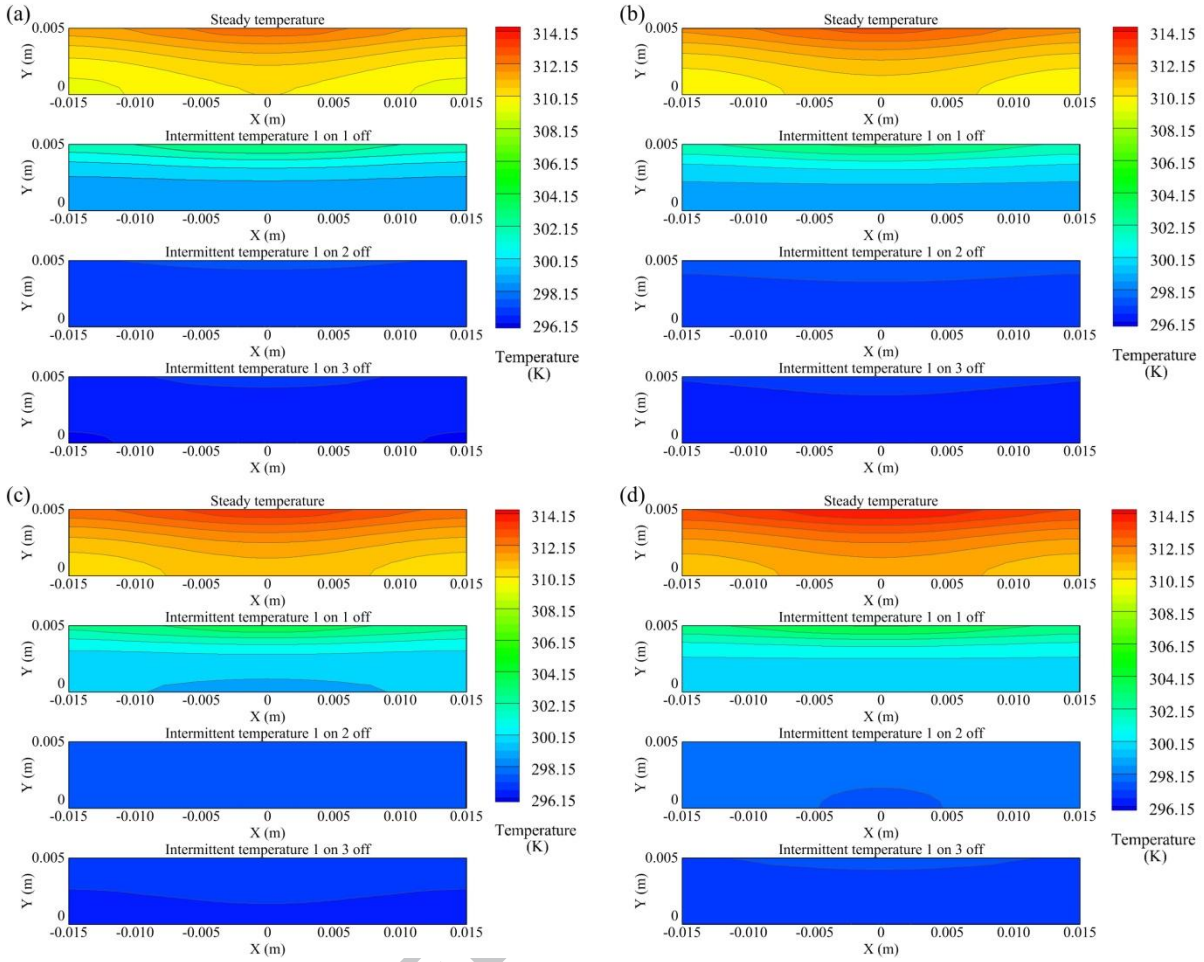

Fig. 5

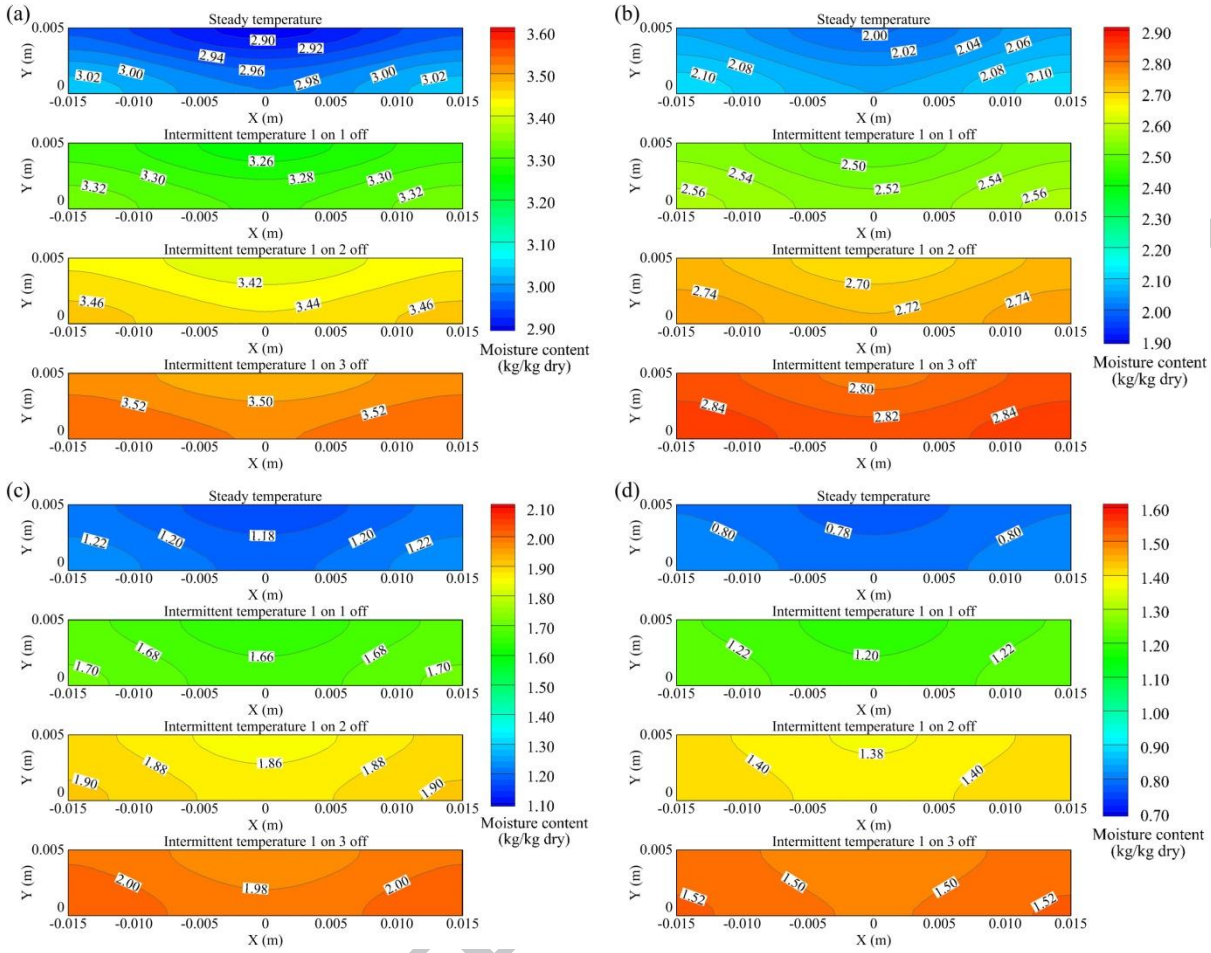

Fig. 6

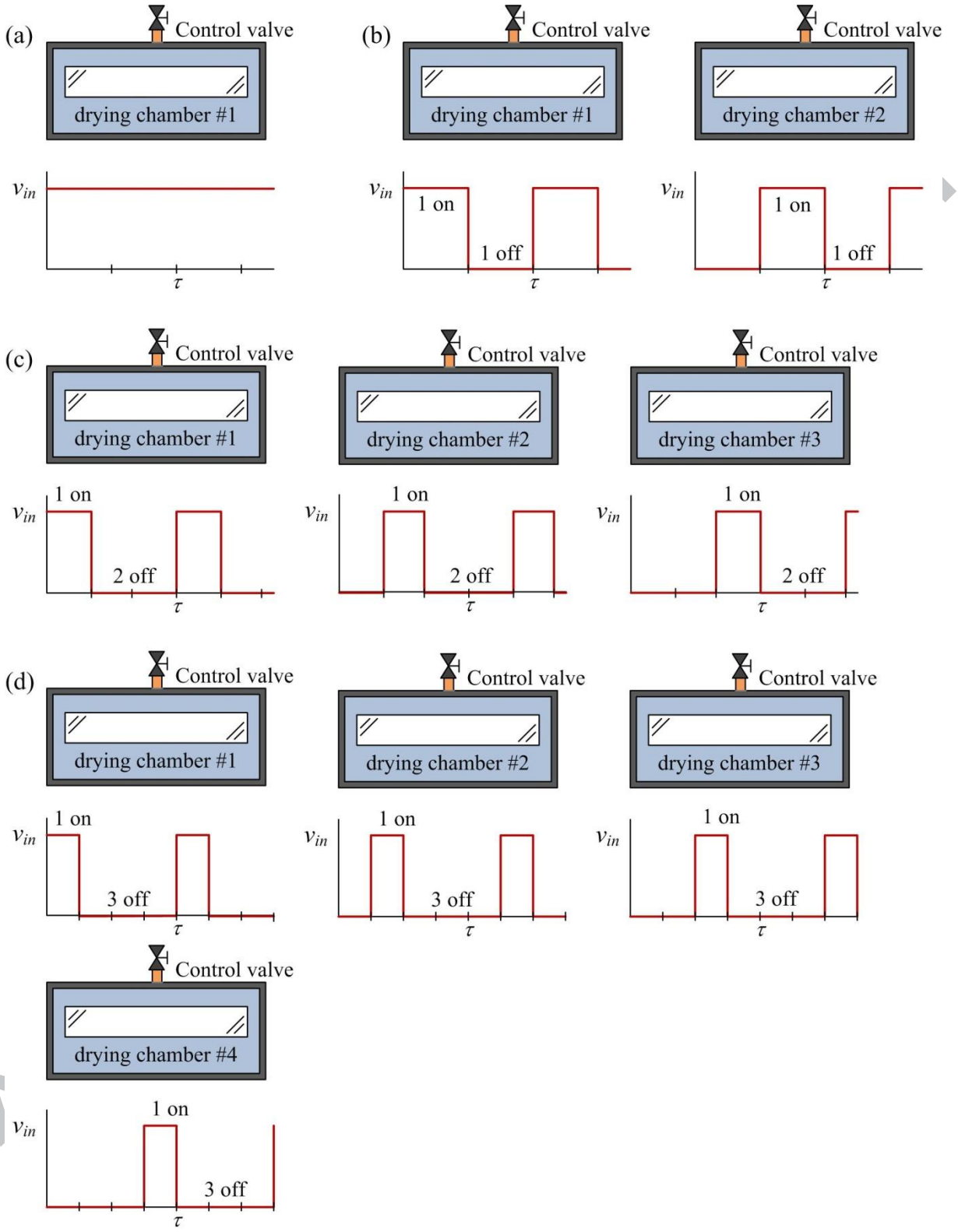

Fig. 7

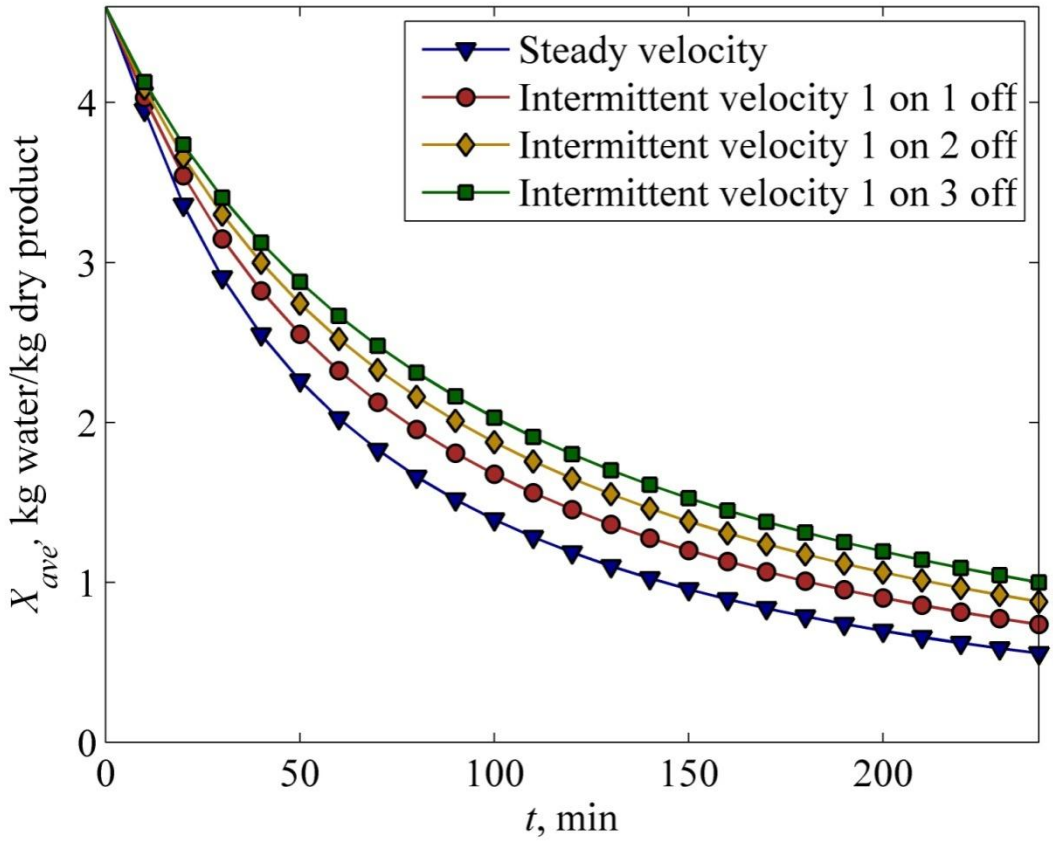

Fig. 8

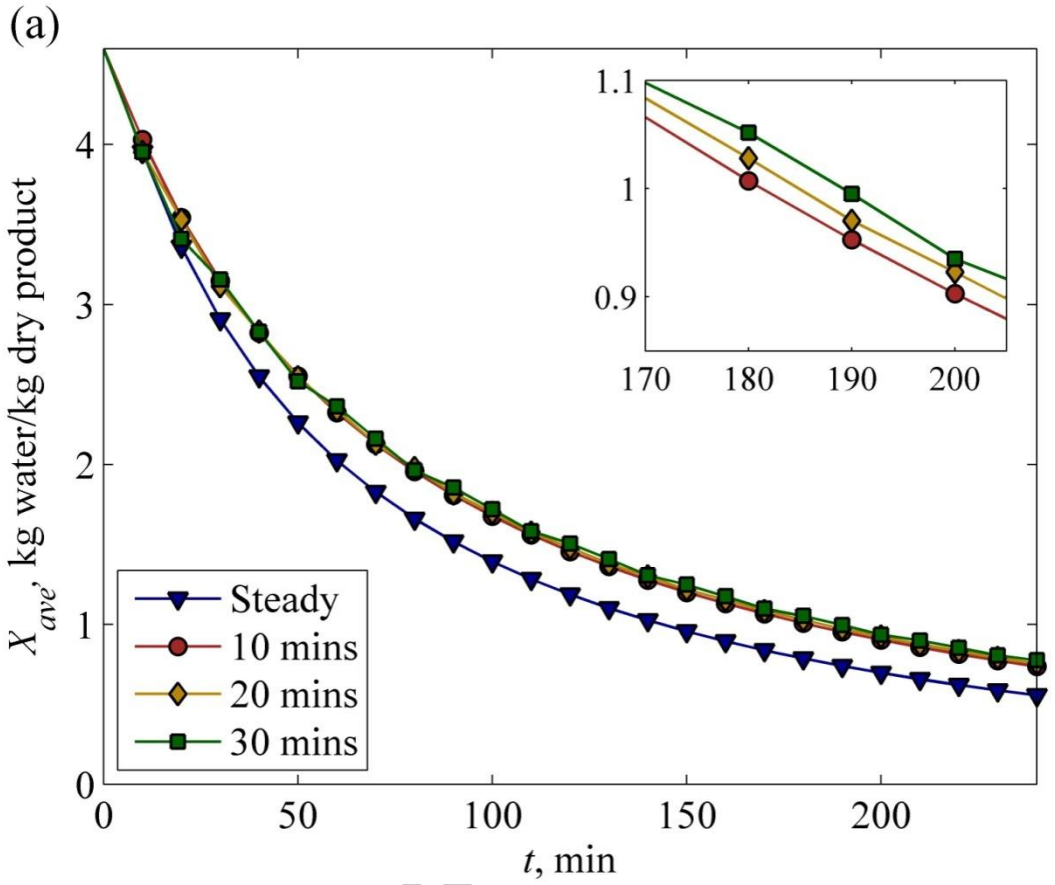

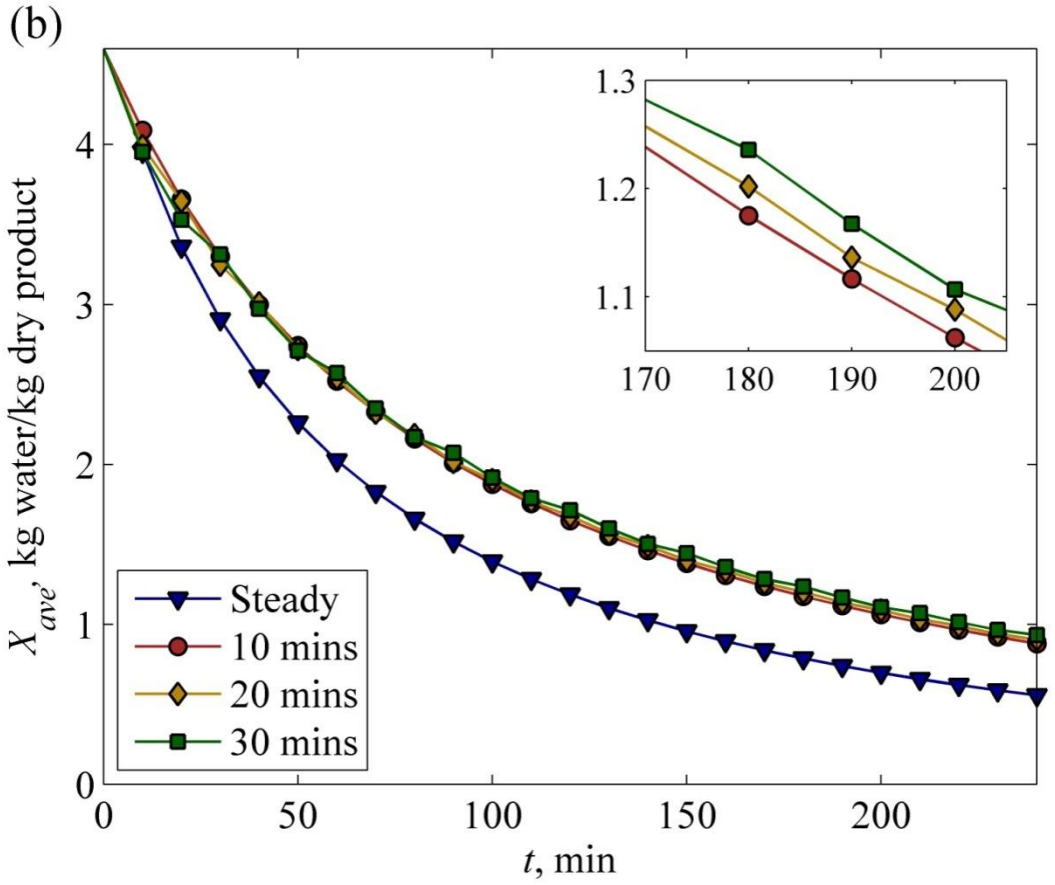

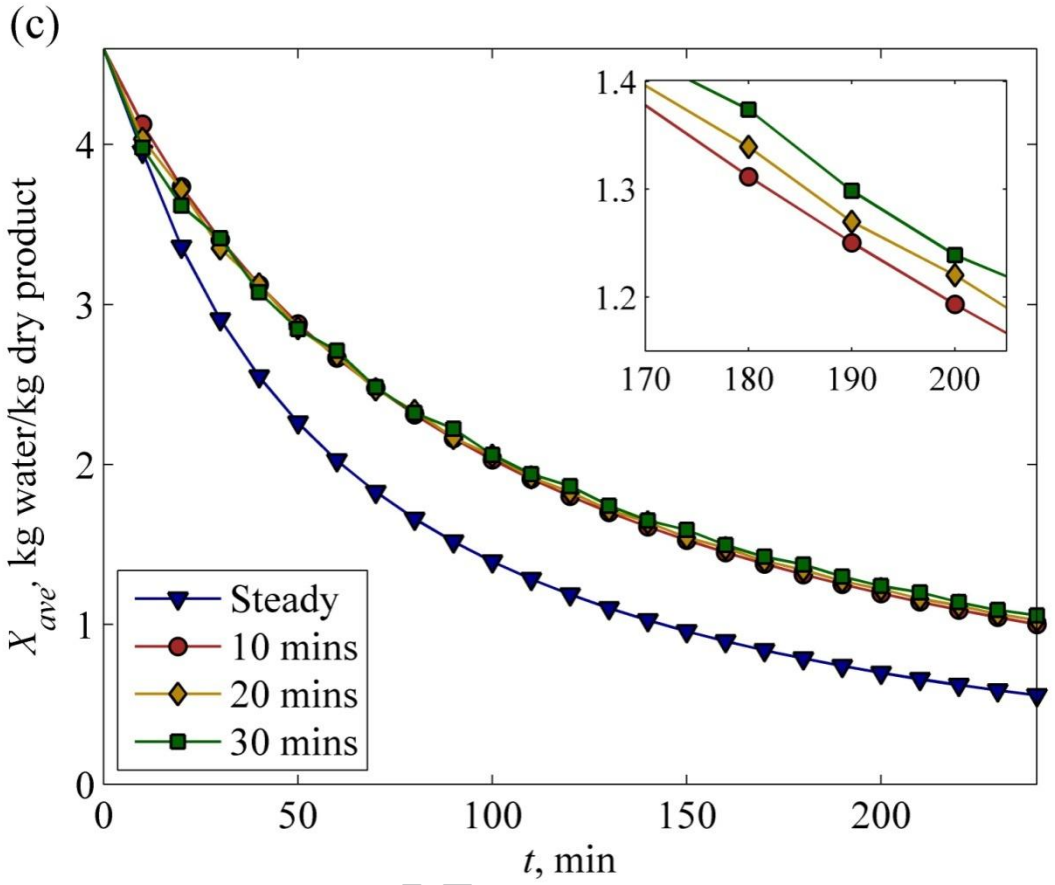

Fig. 9

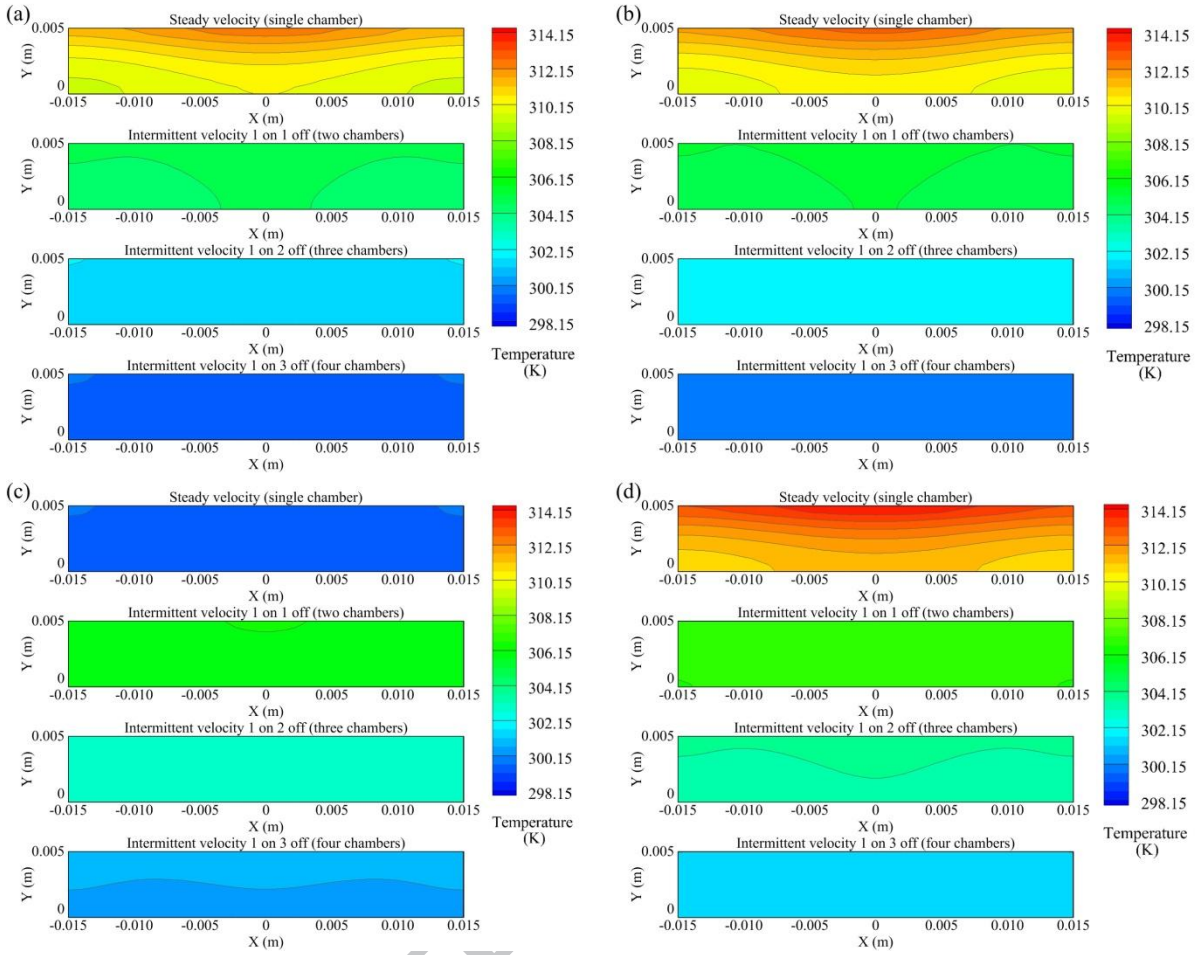

Fig. 10

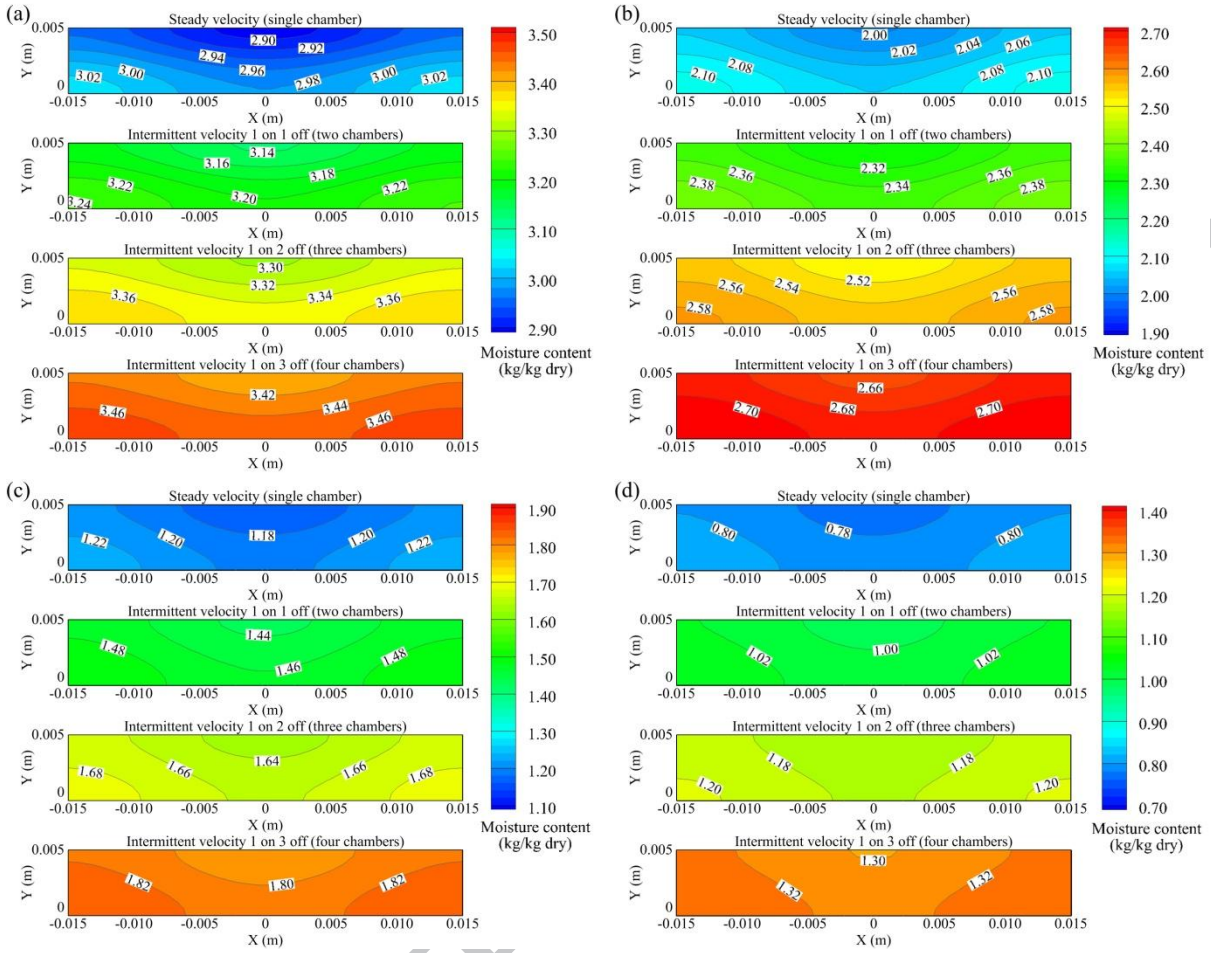

Fig. 11

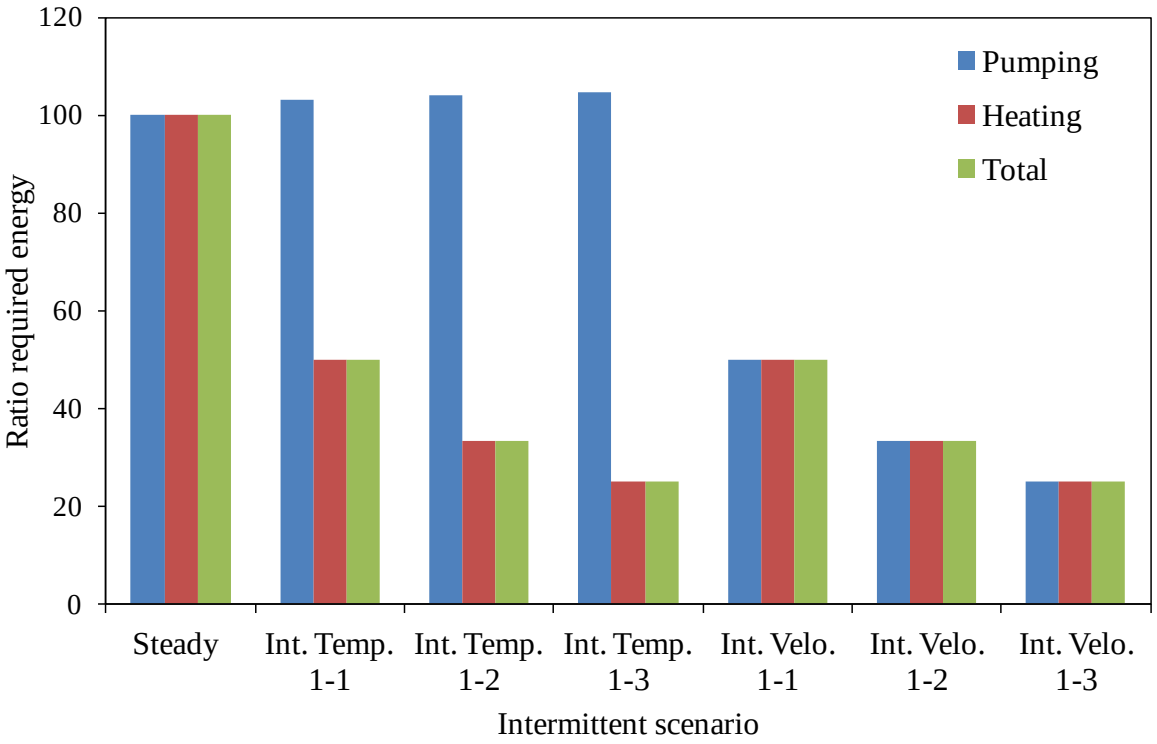

Fig. 12